Desalination and Water Treatment
www.deswater.com

doi: 10.5004/dwt.2017.0487

65 (2017) 435–442
February

Adsorption of Cr(VI) and methyl orange from aqueous solutions by quaternized chitosan immobilized bentonite

Pan Hu, Jing Wang, Ruihua Huang*

College of Chemistry & Pharmacy, Northwest A&F University, Yangling, Shaanxi 712100, China,
emails: hrh20022002@163.com (R. Huang), 1515325595@qq.com (P. Hu), 1396543866@qq.com (J. Wang)

Received 1 May 2016; Accepted 25 November 2016

ABSTRACT

In this study, batch adsorption study was utilized in evaluating the potential suitability of quaternized chitosan immobilized bentonite (BT) as an adsorbent in the adsorption of anionic pollutants, Cr(VI), and methyl orange (MO) from aqueous solutions. The adsorptive behaviors of Cr(VI) and MO were examined as a function of the ratio of quaternized chitosan to BT, adsorbent dosage, solution pH, initial Cr(VI) (or MO) concentration, and contact time. The adsorption equilibrium for both Cr(VI) and MO was reached quickly. Adsorption isotherms for Cr(VI) and MO were well described by the Langmuir isotherm, while the pseudo-second-order kinetic model provided good kinetic data fitting. Furthermore, the results show that this adsorbent exhibited higher adsorption capacity for MO than Cr(VI). It appears that this anionic Cr(VI) favored the electrostatic interactions with this adsorbent while the anionic MO dye may interact with this adsorbent by electrostatic interactions and the hydrogen bonding.

Keywords: Quaternized chitosan; Composite; Methyl orange; Cr(VI); Adsorption

1. Introduction

The heavy metal ions and dyes are two kinds of common pollutants in water body. Their discharge may be toxic or poisonous for human health and animals even at low concentrations. Therefore, the removal of both pollutants from wastewaters is currently one of the most important environmental tasks for research and technology development on water management [1]. Numerous techniques have been utilized for the removal of metals and dyes from solution, which include biological treatment, adsorption, coagulation/flocculation, chemical oxidation, membrane separation, and ion exchange. Among these methods, adsorption has been found to be a superior technique in terms of cost, simplicity of design and operation, effectiveness, and insensitivity to toxic substances [2]. Various materials such as activated carbon [3,4], zeolite [5,6], clay, polymer [7], and nanomaterials [8–10] have been extensively applied for pollutants removal.

Bentonite (BT) clay has great potential as adsorbent due to its large quantities, low-cost, chemical and mechanical stability, high specific surface area, and structural properties [11]. However, BT weakly adsorbs anionic pollutants due to repulsion between the anions and the negative charge on the edge of the BT sheet. Modification of clay through acid treatment, composting with biopolymers, calcinations, functionalization, and pillaring are among several ways that effort has been made by researchers to enhance its usability beyond its application in natural form. Among these modifying methods, the combination of BT and biopolymer gets much attention currently due to high adsorption capacity and regeneration [12]. Quaternized chitosan is a water-soluble derivative of chitosan, and it has several desirable characteristics such as biocompatibility, biodegradability, bioactivity, and non-toxicity. Besides, it contains many active functional groups that serve as efficient sites to bind pollutants, especially anionic pollutants, thus it is itself a good adsorbent due to its unique properties [13]. However, using pure quaternized chitosan as an adsorbent has several disadvantages

* Corresponding author.

such as being costly and low chemical stability. Meanwhile, it is apt to loss due to its water solubility. The combination of quaternized chitosan with other materials like BT is considered to be an effective method [7,14], which could reduce the cost of adsorbents without affecting the adsorption capacity of quaternized chitosan due to the possible intercalation of quaternized chitosan in BT.

In this study, the quaternized chitosan immobilized BT was prepared and characterized. Anionic pollutants Cr(VI) and MO were chosen as a model heavy metal anion and anionic dye, respectively. Chromium, a kind of typical metal elements, exists in the environment in the trivalent state or in the hexavalent state as the Cr(VI) anions: $HCrO_4^-$, CrO_4^{2-}, and $Cr_2O_7^{2-}$. As a strong oxidizing agent and a potential carcinogen, it can have teratogenic and mutagenic effects for plants and animals [15]. Methyl orange (MO) was chosen as a model dye in this study because MO is a common water-soluble azo dye that is widely used in the chemical, textile, and paper industries. MO is an anionic dye and presents a serious environmental hazard [16]. The adsorptive removal of Cr(VI) and MO from aqueous solutions was investigated by a batch method. Experimental parameters affecting the adsorption process such as solution pH, initial Cr(VI) (or MO) concentration, adsorbent dosage, and contact time were studied. Besides, the adsorption isotherms and kinetics were also discussed.

2. Experimental set-up

2.1. Chemicals and reagents

BT powder with a particle size of 200 mesh was acquired from the chemical factory of Shentai, Xinyang, Henan, China. Chitosan [weight-average molecular weight = 100,000 Da, degree of deacetylation = 90%] was purchased from the Sinopharm Group Chemical Reagent Limited Company (China). Quaternized chitosan and *N*-2-hydroxypropyl trimethyl ammonium chloride chitosan were prepared according to our previous literature [17]. Potassium dichromate and MO were obtained from Aladdin (analytical grade). A stock MO solution of 1,000 mg/L was prepared by dissolving 1.00 g of MO in 1 L of distilled water. MO concentrations were measured using a UV–vis spectrometer at a wavelength corresponding to the maximum absorbance for MO: 464 nm.

Stock chromium solution of 1,000 mg/L was prepared by dissolving 2.829 g of potassium dichromate in 1 L of distilled water. The chromium concentration was determined by a double beam UV–vis spectrophotometer (Unicam UV-2) at 540 nm. All other chemical reagents used in this study were of analytical grade. pH value of MO (or Cr(VI)) solutions was adjusted by adding 0.1 M HCl or NaOH solutions.

2.2. Synthesis of quaternized chitosan immobilized BT

Quaternized chitosan (1.5 g) was dissolved in 50 mL of distilled water. About 1 g of BT was added and then stirred for 5 h at room temperature. The mixture was coated in culture vessels and then dried at 60°C to form membranes. Subsequently, these membranes were soaked in ethyl alcohol solution with 2.5 wt% glutaraldehyde (GLA) solution. Cross-linking reaction occurred for 15 h at 60°C and then the complex was washed using distilled water to remove any free GLA and dried in the oven at 60°C for 10 h. After drying, the complex with 100 mesh of particle size was collected and utilized for the batch experiments. The resultant complex was referred to as quaternized chitosan immobilized BT. The interaction among GLA, quaternized chitosan, and BT was depicted in Fig. 1.

2.3. Methods of characterization

The point of zero charge (pH_{pzc}) for the quaternized chitosan immobilized BT was determined according to the method described by the solid addition method [18]. The modified BT (0.1 g) was shaken in 50.00 mL of a 0.01 mol/L NaCl solution for 24 h. The initial pH values (pH_i) were adjusted in the pH range from 1 to 9 by adding appropriate amounts of 0.1 mol/L HCl or 0.1 mol/L NaOH solution. After 24 h of shaking, the final pH values were measured (pH_f). The difference between the initial and final pH (pH_f–pH_i) was plotted against the initial pH (pH_i) and the point at which pH_f–pH_i= 0 was taken as the pH_{pzc}. The FTIR spectra of samples dispersed in KBr disks were recorded at room temperature using a FTIR spectrometer (Shimadzu 4100) in the wave number range of 400–4,000 nm^{-1}.

2.4. Batch adsorption experiments of quaternized chitosan immobilized BT

The adsorption of MO (or Cr(VI)) onto the quaternized chitosan immobilized BT was conducted by a batch procedure. The factors affecting the adsorption of MO and Cr(VI) including the ratio of quaternized chitosan to BT, initial MO (or Cr(VI)) concentration, adsorbent dosage, pH value of initial MO (or Cr(VI)) solutions, and contact time were investigated. The adsorption experiments were carried out in a thermostated shaker. A certain amount of adsorbent was dispersed in 50.00 mL of MO (or Cr(VI)) solution and shaken for predetermined time. After adsorption, the samples were collected by filtration, and the concentrations of the residual MO (or Cr(VI)) in the filtrates were measured.

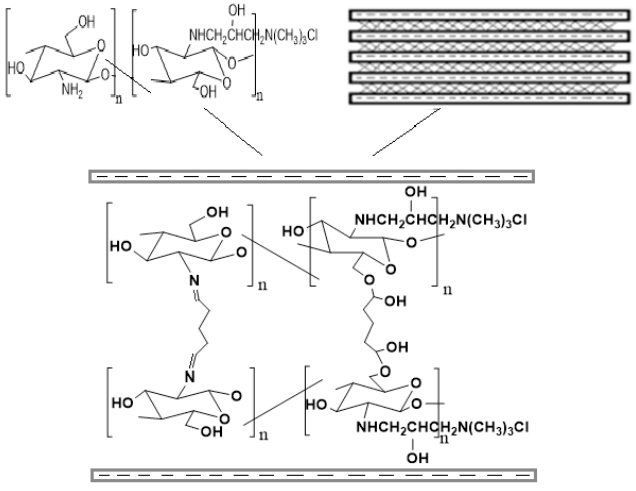

Fig. 1. Scheme for the preparation of quaternized chitosan immobilized bentonite composite.

For kinetic study, MO (or Cr(VI)) solutions with various concentrations were shaken with 0.1 g of adsorbent at 298 K and natural pH for predetermined intervals of time. After the fixed time interval was attained, the adsorbent was separated by filtration and the filtrate obtained was analyzed to determine the MO (or Cr(VI)) concentration and the adsorption capacity was calculated accordingly.

For isotherm study, the adsorption experiments were carried out by shaking MO (or Cr(VI)) with various concentrations and 0.1 g of adsorbent dosage at different temperatures (298, 308, and 318 K). After equilibrium, the adsorbent was separated by filtration and MO (or Cr(VI)) concentration in the filtrate was analyzed.

2.5. Desorption and reusability

The feasibility of reusing the quaternized chitosan immobilized BT adsorbent was investigated by using 0.5 mol/L NaOH as an effluent solution. Typically, 0.1 g adsorbent was first saturated with Cr(VI) (100 mg/L) and MO (200 mg/L) for 1 h. The saturated adsorbent was then separated by filtration and the filtrate was analyzed accordingly. The Cr(VI)- and MO-loaded adsorbents were subsequently agitated for 3 h with 50 mL of 0.5 mol/L NaOH, separated and washed thoroughly with deionized water. The regenerated adsorbents were dried in an oven at 60°C and used in the subsequent adsorption/desorption experiments.

3. Results and discussion

3.1. FTIR spectra analysis

FTIR spectra of BT and cross-linked quaternized chitosan, quaternized chitosan immobilized BT and the samples loaded by MO and Cr(VI) are shown in Figs. 2(A) and (B), respectively. In the spectrum of BT, the peak at 3,623 cm^{-1} was assigned to a stretching band of the inner OH unit within the clay structure, and the peak at 3,455 cm^{-1} was related to the OH vibration of water molecules. The characteristic peaks corresponding to the phyllosilicate structure of BT appeared between 470 and 1,160 cm^{-1}. A broad peak between 1,045 and 1,160 cm^{-1} was attributed to the characteristic stretching vibration of the Si–O [19], and the peak at 525 cm^{-1} belonged to the angular deformation of Si–O in the tetrahedral sheet. The peaks from 915 to 794 cm^{-1} corresponded to the octahedral layers of BT. In the spectrum of cross-linked quaternized chitosan, a broad intense peak near 3,441 cm^{-1} was due to the stretching vibrations of O–H and N–H groups. The peaks at 2,922 and 2,876 cm^{-1} corresponded to the C–H stretching vibrations of the alkyl group. The peaks at 1,643 and 1,564 cm^{-1} were associated to the stretching vibrations of amide and amine groups, respectively. The peak at 1,482 cm^{-1} was attributed to the methyl of the ammonium groups in quaternized chitosan [20].

After BT interacted with cross-linked quaternized chitosan, the intensities of the characteristic peaks of the amine and ammonium groups decreased and was accompanied by slight shifts as compared with those of cross-linked quaternized chitosan The intensities of the characteristic peaks of BT changed and this was accompanied by the changes in the positions of these peaks in comparison with the spectrum

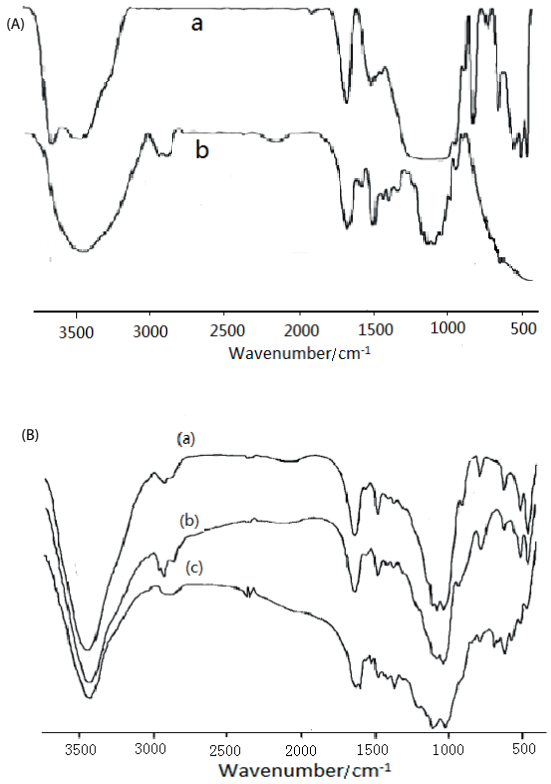

Fig. 2. (A) FTIR patterns of bentonite (a) and cross-linked quaternized chitosan (b). (B) FTIR spectra of quaternized chitosan immobilized bentonite (a) and the samples loaded by Cr(VI) (b) and MO (c).

of BT. These results indicated that the amine and ammonium groups in cross-linked quaternized chitosan mainly participated in the reaction with BT.

After the complex was loaded by Cr(VI), the peak attributed to the stretching vibration of amide group shifted from 1,642 to 1,638 cm^{-1}, while the peak at 1,486 cm^{-1} was shifted to 1,489 cm^{-1} with the decreased intensities. These changes indicated the quaternary ammonium and amide groups were involved in the adsorption of Cr(VI). Meanwhile, the characteristic peaks of BT were changed slightly whether in the intensities or the positions as compared with that of the complex before Cr(VI) adsorption. However, after the complex was loaded by MO, the characteristic peaks of the amine and quaternary ammonium groups decreased in the intensities and even disappeared, and the intensities and positions of the characteristic peaks of BT were different from those of the complex before MO adsorption. These results indicated the quaternary ammonium and amide groups from quaternized chitosan as well as hydroxyl groups in BT were related to MO adsorption. Besides, a new peak at 1,372 cm^{-1} attributed to aromatic nitro compound was detected, indicating the presence of MO molecules on the adsorbent surface [12]. Therefore, the mechanism for Cr(VI) adsorption was mainly the electrostatic interaction, while the mechanism for MO adsorption involved the electrostatic interaction and the hydrogen bonds between this adsorbent and MO.

3.2. Effect of the ratio of quaternized chitosan to BT on Cr(VI) (or MO) adsorption

To investigate the effect of the ratio of quaternized chitosan to BT on Cr(VI) (or MO) adsorption, this ratio changed from 0.3 to 1.8. The adsorption experiments were conducted at 298 K using 200 mg/L MO and 100 mg/L Cr(VI) solutions. As shown in Fig. 3, single BT had low removal toward both Cr(VI) and MO, while single cross-linked quaternized chitosan showed relatively high removal toward Cr(VI) and MO. The removal of Cr(VI) and MO increased significantly when the ratio of quaternized chitosan to BT in this complex increased from 0 to 1.5. Beyond 1.5, increasing this ratio had no significant effect on the adsorption of Cr(VI) or MO. An increase in this ratio indicates an increase in the content of quaternized chitosan or a decrease in BT content. Therefore, the quaternized chitosan acted as an important factor for Cr(VI) and MO adsorption. Considering the cost of quaternized chitosan and the removal of Cr(VI) and MO together, the ratio of quaternized chitosan to BT was fixed at 1.5 in this complex and used for the preparation of adsorbents.

3.3. Effect of adsorbent dosage on Cr(VI) (or MO) adsorption

For this test, the adsorption experiments were performed at 298 K using 200 mg/L MO and 100 mg/L Cr(VI) solutions. As shown in Fig. 4, the removal increased from 51.2% to 90.6% for Cr(VI) and from 79.0% to 97.4% for MO, respectively, when the adsorbent dosage increased from 0.05 to 0.1 g. This increase in removal may be attributed to the increasing sites available for adsorption as increasing adsorbent dosage [21]. However, the removal remained almost constant beyond 0.1 g of adsorbent dosage. The constant removal resulted from the adsorption of Cr(VI) and MO saturated. This study utilized 0.1 g of adsorbent dosage for the following experiments.

3.4. Effect of initial MO (or Cr(VI)) concentrations on MO (or Cr(VI)) adsorption

The adsorption experiments were carried out in single and binary systems at 298 K. 0.1 g of adsorbent was added to 50 mL aqueous solution and continuously agitated at 200 rpm for 60 min. The results were presented in Fig. 5, the removal toward Cr(VI) decreased from 96.4% to 47.3% with increasing initial Cr(VI) concentration from 50 to 300 mg/L. This decrease in removal can be explained by the fact that at low concentrations, the ratio of available sites to initial concentration was high, thus the removal enhanced, while at high concentrations, this ratio became low, and these sites was not enough for the adsorption of Cr(VI) ions, thus the removal decreased [22]. However, the removal toward MO had no significant decrease with increasing initial MO concentrations, this trend may be attributed to the sufficient sites for MO adsorption in the range of MO concentrations tested.

3.5. Effect of pH value of MO (or Cr(VI)) solutions on MO (or Cr(VI)) adsorption

The initial pH of a system is known to be an important parameter for adsorption due to the influence of pH value of solutions on the adsorbent surface properties and existing forms of adsorbates. To investigate the effect of pH value on MO (or Cr(VI)) adsorption, the adsorption experiments were performed at 298 K. 0.1 g of adsorbent was added to 50 mL 200 mg/L MO solution (or 100 mg/L Cr(VI)) and continuously agitated at 200 rpm for 60 min. Fig. 6 shows that the removal toward Cr(VI) and MO decreased obviously with an increase in pH values of solutions from 3 to 11. This indicates that the adsorption of Cr(VI) and MO on this adsorbent was favored at lower pH value. The pH dependence of Cr(VI) (or MO) adsorption can largely be related to the type and ionic state of these functional groups in adsorbent and also on the existing forms of Cr(VI) (or MO) in solution. As we know, the existing form of Cr(VI) is greatly dependent upon the pH and concentration of the solution. At pH between 3 and 6, $Cr_2O_7^{2-}$ and chromate (CrO_4^{2-}) exist in equilibrium and under alkaline conditions (pH > 8), it exists predominantly as $HCrO_4^-$ [23]. However, MO is attributed to anionic dye, and the sulfonate groups of MO (–SO_3Na) were dissociated and converted to anionic dye ions –SO_3^- in aqueous solution. The value for pH_{pzc} of this adsorbent was obtained at 6.5 or so (see Fig. 7). The surface of the adsorbent will be negatively

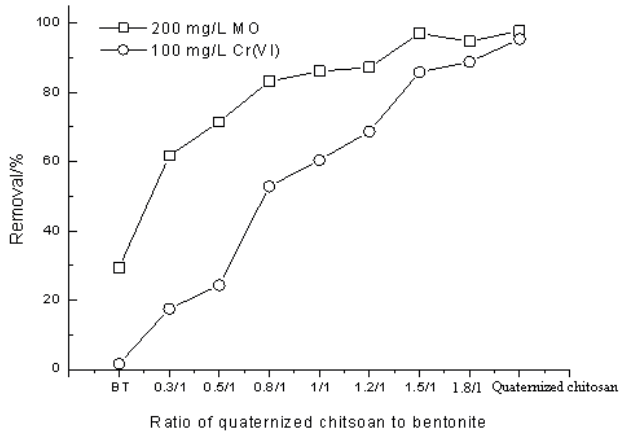

Fig. 3. Effect of the ratio of quaternized chitosan to bentonite on Cr(VI) (or MO) adsorption.

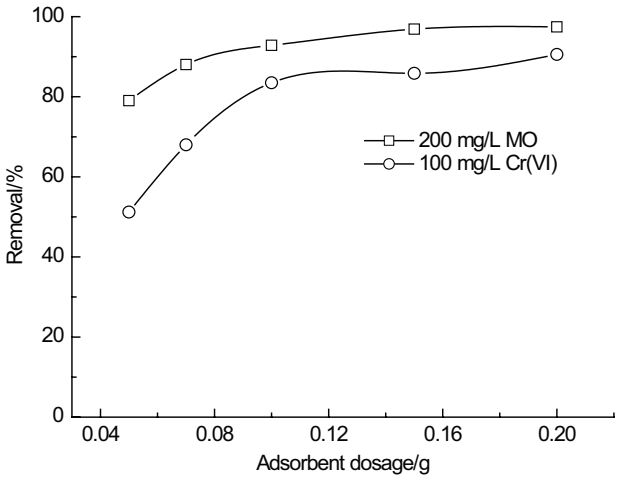

Fig. 4. Effect of adsorbent dosage on Cr(VI) (or MO) adsorption.

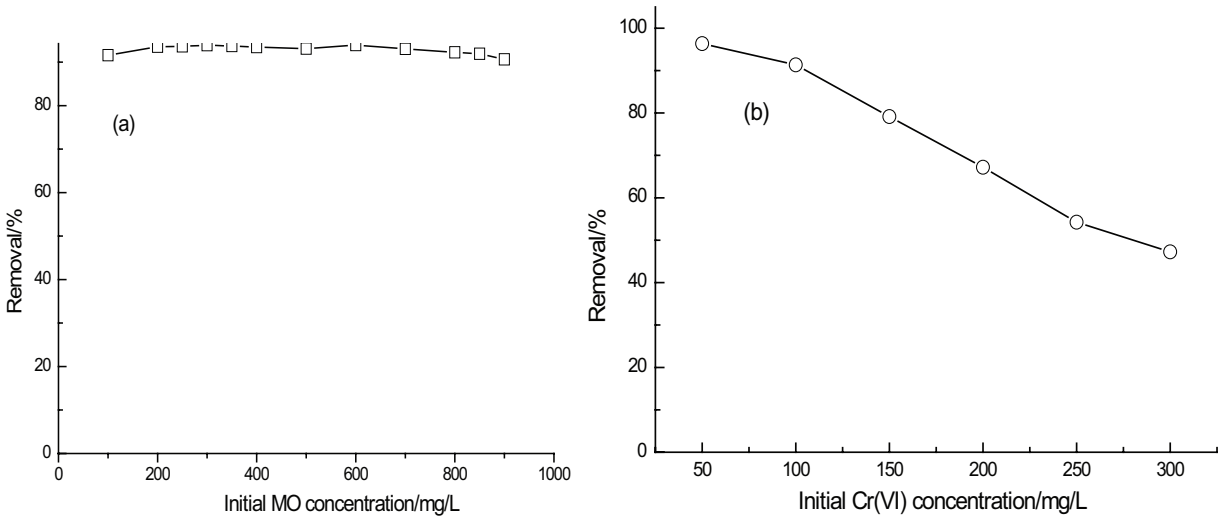

Fig. 5. Effect of initial MO (or Cr(VI)) concentrations on MO (or Cr(VI)) adsorption.

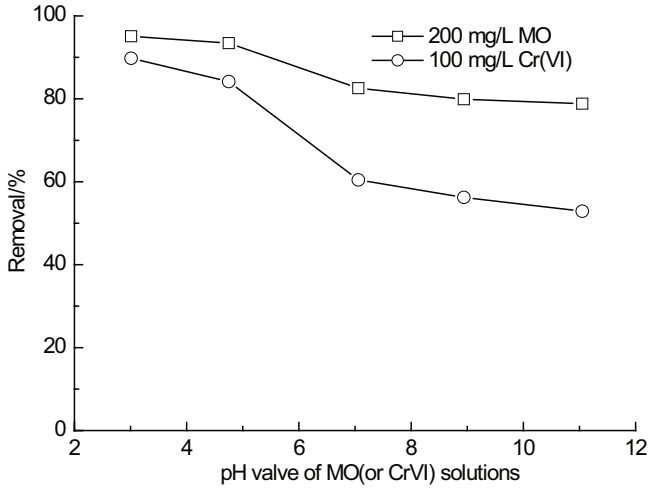

Fig. 6. Effect of pH value of MO (or Cr(VI)) solutions on MO (or Cr(VI)) adsorption.

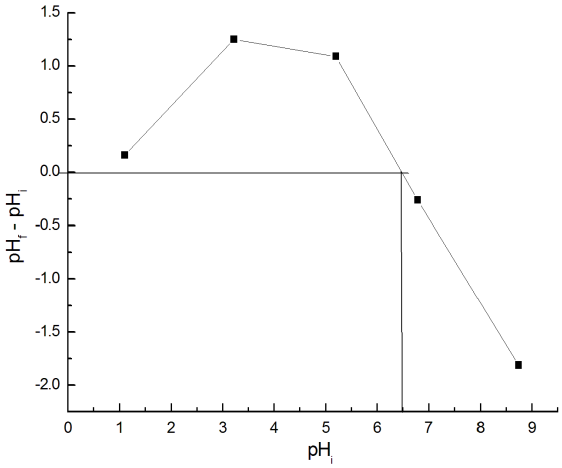

Fig. 7. Determination of pH_{pzc} of quaternized chitosan immobilized bentonite.

charged above pH_{pzc} and positively charged below pH_{pzc}. At low pH values (<pH_{pzc}), the surface of this adsorbent was positively charged, which facilitated the adsorption of Cr(VI) (or MO) adsorption due to the electrostatic attraction between Cr(VI) ions (or MO) and positively charged adsorption sites, thereby increasing Cr(VI) (or MO) adsorption. With increasing pH (>pH_{pzc}), a decline in removal may be ascribed to the repulsive force between the negatively charged surface of this adsorbent and Cr(VI) ions (or MO) as well as the competitive adsorption of abundant OH^- ions.

3.6. Effect of contact time on Cr(VI) (or MO) adsorption

The effect of contact time on the adsorption of Cr(VI) (or MO) by this adsorbent was studied using Cr(VI) (or MO) solutions with different concentrations, and the results are shown in Fig. 8. For whether MO or Cr(VI), the adsorption was initially rapid, and then slowed. The rapid adsorption at the initial stage may be attributed to a large number of vacant surface sites available for adsorption. The adsorptive sites became less and less during the process of adsorption, and the remaining vacant surface sites were difficult to occupy because of the repulsive forces between the dye molecules (or Cr(VI)) on the adsorbent and the bulk phase. Besides, the longer time was required for equilibrium with increasing MO concentrations, while the adsorption for Cr(VI) showed the contrary trend. The equilibrium time for MO and Cr(VI) adsorption was 60 and 30 min, respectively, in the range of MO (or Cr(VI)) concentrations tested.

The adsorption kinetics may be described by the pseudo-second-order model, which is generally given as follows:

$$\frac{t}{q_t} = \frac{1}{k_2 q_e^2} + \frac{1}{q_e} t \quad (1)$$

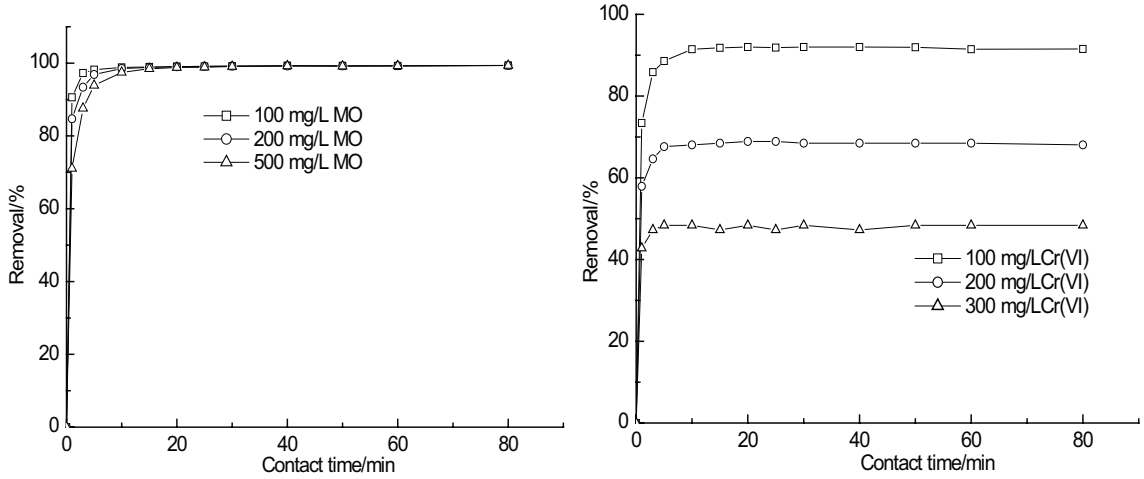

Fig. 8. Effect of contact time on Cr(VI) (or MO) adsorption.

where k_2 is the rate constant of pseudo-second-order adsorption (g/(mg min)). The slope of the plot of t/q_t vs. t gives the value for the calculated adsorption capacity at equilibrium ($q_{e,cal}$), whereas the intercept gives the value for the rate constant (k_2). The values of k_2, correlation coefficients, $q_{e,cal}$ and $q_{e,exp}$ are listed in Table 1. From Table 1, the pseudo-second-order model had high correlation coefficient ($R^2 > 0.9999$). Besides, the $q_{e,cal}$ from the pseudo-second-order model was very closely similar to the $q_{e,exp}$ whether for MO or for Cr(VI) adsorption by this adsorbent. Therefore, the pseudo-second-order model may be applied to predict the kinetic behavior of MO and Cr(VI) adsorption. In addition, the values of k_2 for the adsorption of MO were found to decrease with the increase of MO concentration, suggesting that the time required for equilibrium at high MO concentration was relatively prolonged. However, the values of k_2 for Cr(VI) adsorption increased with an increase in Cr(VI) concentration, suggesting that the shorter time was required for equilibrium at high Cr(VI) concentration. These results were consistent with the above phenomena mentioned.

3.7. Adsorption isotherms

The equilibrium sorption data of MO and Cr(VI) on this adsorbent were investigated using the adsorption isotherm models via, Langmuir and Freundlich. The linear form of Langmuir equation is given as follows:

$$\frac{C_e}{q_e} = \frac{1}{Qb} + \frac{C_e}{Q} \tag{2}$$

where C_e is the equilibrium concentration (mg/L); q_e is the amount adsorbed at equilibrium (mg/g); Q is the maximum amount of adsorption with complete monolayer coverage on the adsorbent surface (mg/g); and b is the Langmuir constant, which is related to the energy of adsorption (L/mg). From the linear plots of C_e/q_e against C_e, Q, and b values can be calculated from the slope and intercept, respectively.

The linear form of Freundlich equation is expressed as follows:

Table 1
Pseudo-second-order parameters of MO and Cr(VI) adsorption by the quaternized chitosan immobilized bentonite

Adsorbates	Concentration (mg/L)	k_2	$q_{e,cal}$	$q_{e,exp}$	R^2
MO	100	0.277	49.70	49.63	1.0000
	300	0.049	149.2	148.9	1.0000
	500	0.014	249.4	248.2	1.0000
Cr(VI)	100	0.308	45.89	45.00	0.9999
	200	0.387	68.26	68.46	0.9999
	300	0.412	72.62	72.56	0.9999

$$\log q_e = \log K_f + \frac{1}{n}\log C_e \tag{3}$$

where C_e is the equilibrium concentration (mg/L) and q_e is the amount adsorbed at equilibrium (mg/g). K_f [(mg/g)(L/mg)$^{1/}$n] and n are Freundlich constants related to adsorption capacity and heterogeneity factor, respectively. K_f and n values can be calculated from the intercept and slope of the linear plots between logC_e and logq_e for the removal of both adsorbates using this adsorbent.

The isotherm parameters and the values correlation coefficient were given in Table 2. From the isotherm data, the suitable adsorption isotherm for the sorption of MO and Cr(VI) was found to be Langmuir isotherm and hence it could be concluded that the monolayer adsorption on the homogeneous surface of this adsorbent occurred. Meanwhile, for MO, the value of Q decreased with the increasing temperature, suggesting that the adsorption of MO onto this adsorbent was an exothermic process. However, the adsorption of Cr(VI) onto this adsorbent was not affected by temperature in the temperature range of the study. Some adsorbents with their respective adsorption capacities [24–33] for the removal of MO (or Cr(VI)) have been given in Table 3. It is evident that this adsorbent had a relatively high adsorption capacity for both MO and Cr(VI). It indicates that this adsorbent showed a potential for the removal of MO and Cr(VI) from aqueous solutions.

Table 2
Langmuir and Freundlich isotherm parameters of MO and Cr(VI) adsorption by the quaternized chitosan immobilized bentonite

Isotherm models		Langmuir			Freundlich		
Adsorbates	Temperature (K)	Q (mg/g)	b (L/mg)	R^2	K_f ([(mg/g)(L/mg)$^{1/n}$)	n	R^2
MO	298	699.3	0.125	0.9998	99.81	1.706	0.9952
	308	657.9	0.144	0.9993	106.0	1.785	0.9908
	318	633.0	0.150	0.9997	107.8	1.855	0.9934
Cr(VI)	298	72.36	0.190	0.9996	23.98	4.287	0.9612
	308	73.21	0.188	0.9998	23.79	4.204	0.9577
	318	73.42	0.146	0.9994	22.59	4.108	0.9755

Table 3
Adsorption capacities for Cr(VI) and MO by various adsorbents

Adsorbent	Adsorption capacity (mg/g)		References
	Cr(VI)	MO	
Nanostructured proton containing δ-MnO_2	–	427	[24]
Poly-2-hydroxyethy methacrylate-chitosan functionalized-multi-walled carbon nanotube	–	400	[25]
CuO/NaA zeolite	–	79.49	[26]
Magnetic chitosan beads	–	779	[27]
Surfactant modified silkworm exuviae	–	87.03	[28]
Amphoteric functionalized mesoporous silica	171.86	–	[29]
Modified kaolin clay	91.10	–	[30]
β-cyclodextrin/ ethylenediamine/magnetic	68.41	–	[31]
Graphene nanosheets	43	–	[32]
Activated carbon/Chitosan composite	53.54	–	[33]
Quaternized chitosan immobilized bentonite	72.36	699.3	This work

3.8. Desorption study

The reusability of adsorbents is of great importance in lowering the cost of wastewater treatment. For quaternized chitosan immobilized BT, 0.5 mol/L NaOH was selected as the regeneration agent for desorption of Cr(VI) and MO adhering on the composite sorbent. Three cycles of adsorption–desorption studies were carried out accordingly. The removal for MO was as high as 96% during these three cycles (Fig. 9). As compared with the fresh adsorbent, the removal decreased slightly. However, the removal decreased from 91.5% to 71.1% after these cycles. Over three adsorption–desorption process, the removal for Cr(VI) reduced dramatically. These results suggested that the removal was affected by the number of cycles for different adsorbates to some degree.

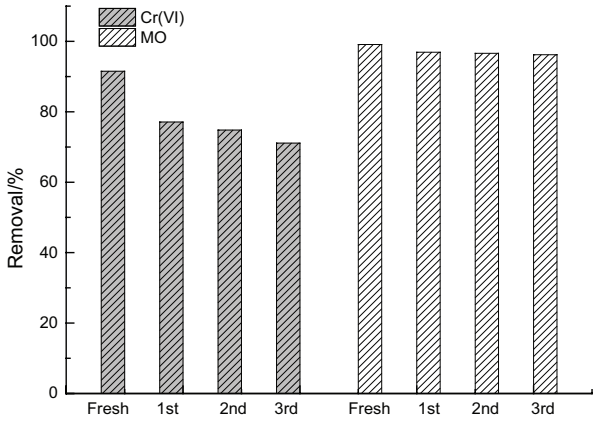

Fig. 9. Regeneration of quaternized chitosan immobilized bentonite.

4. Conclusions

The quaternized chitosan immobilized BT was found to be effective for the removal of MO and Cr(VI). This adsorbent showed higher adsorption capacity at the acidic pH. In adsorption of both MO and Cr(VI) studies, the adsorption equilibrium for Cr(VI) and MO was reached quickly. The kinetic data were well fitted with the pseudo-second-order model. The adsorption data were described by the Langmuir adsorption isotherm which indicates the homogeneous nature of adsorption. The monolayer adsorption capacities were obtained at 699.3 mg/g for MO and 72.4 mg/g for Cr(VI). Besides, this adsorbent showed stronger binding for MO as compared with Cr(VI). Electrostatic interaction between the anions and the positive functional groups in this adsorbent was the mechanism behind the adsorption. However, for MO adsorption, the hydrogen bonding also existed.

References

[1] R. Tovar-Gomez, D.A. Rivera-Ramírez, V. Hernandez-Montoya, A. Bonilla-Petriciolet, C.J. Durán-Valle, M.A. Montes-Morán, Synergic adsorption in the simultaneous removal of acid blue 25 and heavy metals from water using a $Ca(PO_3)_2$-modified carbon, J. Hazard. Mater., 199 (2012) 290–300.

[2] G.Z. Kyzas, N.K. Lazaridis, M. Kostoglou, On the simultaneous adsorption of a reactive dye and hexavalent chromium from aqueous solutions onto grafted chitosan, J. Colloid Interface Sci., 407 (2013) 432–441.

[3] A.M. Youssef, A.I. Ahmed, M.I. Amin, U.A. El-Banna, Adsorption of lead by activated carbon developed from rice husk, Desal. Wat. Treat., 54 (2015) 1694–1707.
[4] J. Shou, M. Qiu, Adsorption of copper ions onto activated carbon from capsicum straw, Desal. Wat. Treat., 57 (2016) 353–359.
[5] M. Zieliński, M. Zielińska, M. Dębowski, Ammonium removal on zeolite modified by ultrasound, Desal. Wat. Treat., 57 (2016) 8748–8753.
[6] F. Aydın Temel, A. Kuleyin, Ammonium removal from landfill leachate using natural zeolite: kinetic, equilibrium, and thermodynamic studies, Desal. Wat. Treat., 57 (2016) 23873–23892.
[7] X. Li, Y. Han, Y. Ling, X. Wang, R. Sun, Assembly of layered silicate loaded quaternized chitosan/reduced graphene oxide composites as efficient absorbents for double-stranded DNA, ACS Sustain. Chem. Eng., 3 (2015) 1846–1852.
[8] J. Luo, G. Han, M. Xie, Z. Cai, X. Wang, Quaternized chitosan/montmorillonite nanocomposite resin and its adsorption behavior, Iran. Polym. J., 24 (2015) 531–539.
[9] H.R. Mahmoud, S.M. Ibrahim, S.A. El-Molla, Textile dye removal from aqueous solutions using cheap MgO nanomaterials: adsorption kinetics, isotherm studies and thermodynamics, Adv. Powder Technol., 27 (2016) 223–231.
[10] K.B. Tan, M. Vakili, B.A. Horri, P.E. Poh, A.Z. Abdullah, B. Salamatinia, Adsorption of dyes by nanomaterials: recent developments and adsorption mechanisms, Sep. Purif. Technol., 150 (2015) 229–242.
[11] J. Nones, H.G. Riella, A.G. Trentin, J. Nones, Effects of bentonite on different cell types: a brief review, Appl. Clay Sci., 105 (2015) 225–230.
[12] M. Auta, B.H. Hameed, Chitosan–clay composite as highly effective and low-cost adsorbent for batch and fixed-bed adsorption of methylene blue, Chem. Eng. J., 237 (2014) 352–361.
[13] A. Sowmya, S. Meenakshi, A novel quaternized chitosan–melamine–glutaraldehyde resin for the removal of nitrate and phosphate anions, Int. J. Biol. Macromol., 64 (2014) 224–232.
[14] M. Lai, P. Liu, H. Lin, Y. Luo, H. Li, X. Wang, R. Sun, Interaction between chitosan-based clay nanocomposites and cellulose in a chemical pulp suspension, Carbohydr. Polym., 137 (2016) 375–381.
[15] A. Gładysz-Płaska, M. Majdan, S. Pikus, D. Sternik, Simultaneous adsorption of chromium (VI) and phenol on natural red clay modified by HDTMA, Chem. Eng. J., 179 (2012) 140–150.
[16] T. Kou, Y. Wang, C. Zhang, J. Sun, Z. Zhang, Adsorption behavior of methyl orange onto nanoporous core–shell Cu@Cu_2O nanocomposite, Chem. Eng. J., 223 (2013) 76–83.
[17] H.B. Senturk, D. Ozdes, A. Gundogdu, C. Duran, M. Soylak, Removal of phenol from aqueous solutions by adsorption onto organomodified Tirebolu bentonite: equilibrium, kinetic and thermodynamic study, J. Hazard. Mater., 172 (2009) 353–362.
[18] P. Monvisade, P. Siriphannon, Chitosan intercalated montmorillonite: preparation, characterization and cationic dye adsorption, Appl. Clay Sci., 42 (2009) 427–431.
[19] W.A. Zhang, D.Z. Chen, H.Y. Xu, X.F. Shen, Y.E. Fang, Influence of four different types of organophilic clay on the morphology and thermal properties of polystyrene/clay nanocomposites prepared by using the γ-ray irradiation technique, Eur. Polym. J., 39 (2003) 2323–2328.
[20] Y. Ling, X. Zeng, W. Tan, J. Luo, S. Liu, Quaternized chitosan/rectorite/AgNP nanocomposite catalyst for reduction of 4-nitrophenol, J. Alloy Compd., 647 (2015) 463–470.
[21] A. Bhatnagar, E. Kumar, M. Sillanpää, Fluoride removal from water by adsorption—a review, Chem. Eng. J., 171 (2011) 811–840.
[22] N. Viswanathan, C.S. Sundaram, S. Meenakshi, Sorption behaviour of fluoride on carboxylated cross-linked chitosan beads, Colloids Surf., B, 68 (2009) 48–54.
[23] R. Ansari, N.K. Fahim, Application of polypyrrole coated on wood sawdust for removal of Cr(VI) ion from aqueous solutions, React. Funct. Polym., 67 (2007) 367–374.
[24] Y. Liu, C. Luo, J. Sun, H. Li, Z. Sun, S. Yan, Enhanced adsorption removal of methyl orange from aqueous solution by nanostructured proton-containing δ-MnO_2, J. Mater. Chem. A, 3 (2015) 5674- 5682.
[25] H. Mahmoodian, O. Moradi, B. Shariatzadeha, T.A. Salehf, I. Tyagi, A. Maity, M. Asif, V.K. Gupta, Enhanced removal of methyl orange from aqueous solutions by poly HEMA-chitosan-MWCNT nanocomposite, J. Mol. Liq., 202 (2015) 189–198.
[26] E.H. Mekatel, S. Amokrane, A. Aid, D. Nibou, M. Trari, Adsorption of methyl orange on nanoparticles of a synthetic zeolite NaA/CuO, C.R. Chim., 18 (2015) 336–344.
[27] L. Obeid, A. Bée, D. Talbot, S.B. Jaafar, V. Dupuis, S. Abramson, V. Cabuil, M. Welschbillig, Chitosan/maghemite composite: a magsorbent for the adsorption of methyl orange, J. Colloid Interface Sci., 410 (2013) 52–58.
[28] H. Chen, J. Zhao, J. Wu, G. Dai, Isotherm, thermodynamic, kinetics and adsorption mechanism studies of methyl orange by surfactant modified silkworm exuviae, J. Hazard. Mater., 192 (2011) 246–254.
[29] Q. Wu, R. You, Q. Lv, Y. Xu, W. You, Y. Yu, Efficient simultaneous removal of Cu(II) and $Cr_2O_7^{2-}$ from aqueous solution by a renewable amphoteric functionalized mesoporous silica, Chem. Eng. J., 281 (2015) 491–501.
[30] L. Deng, Z. Shi, B. Li, L. Yang, L. Luo, X. Yang, Adsorption of Cr(VI) and phosphate on Mg–Al hydrotalcite supported kaolin clay prepared by ultrasound-assisted coprecipitation method using batch and fixed-bed systems, Ind. Eng. Chem. Res., 53 (2014) 7746–7757.
[31] H. Wang, Y.G. Liu, G.M. Zeng, X.J. Hu, X. Hu, T.T. Li, H.Y. Li, Y.Q. Wang, L.H. Jiang, Grafting of β-cyclodextrin to magnetic graphene oxide via ethylenediamine and application for Cr(VI) removal, Carbohydr. Polym., 113 (2014) 166–173.
[32] H. Jabeen, V. Chandra, S. Jung, J.W. Lee, K.S. Kim, S.B. Kim, Enhanced Cr(VI) removal using iron nanoparticle decorated graphene, Nanoscale, 3 (2011) 3583–3585.
[33] R. Huang, B. Yang, Q. Liu, Y. Liu, Simultaneous adsorption of aniline and Cr(VI) ion by activated carbon/chitosan composite, J. Appl. Polym. Sci., 131 (2014) 1001–1007.